Inorganic Chemistry

Article

pubs.acs.org/IC

Na_2TeS_3, Na_2TeSe_3-*mP*24, and Na_2TeSe_3-*mC*48: Crystal Structures and Optical and Electrical Properties of Sodium Chalcogenidotellurates(IV)

Constantin Pompe, Christian Preitschaft, Richard Weihrich, and Arno Pfitzner*

Institut für Anorganische Chemie, Universität Regensburg, 93040 Regensburg, Germany

Supporting Information

ABSTRACT: Pure samples of Na_2TeS_3 and Na_2TeSe_3 were synthesized by the reactions of stoichiometric amounts of the elements Na, Te, and Q (Q = S, Se) in the ratio 2:1:3. Both compounds are highly air- and moisture-sensitive. The crystal structures were determined by single-crystal X-ray diffraction. Yellow Na_2TeS_3 crystallizes in the space group $P2_1/c$. Na_2TeSe_3 exists in a low-temperature modification (Na_2TeSe_3-*mP*24, space group $P2_1/c$) and a high-temperature modification (Na_2TeSe_3-*mC*48, space group $C2/c$); both modifications are red. Density functional theory calculations confirmed the coexistence of both modifications of Na_2TeSe_3 because they are very close in energy (ΔE = 0.18 kJ mol^{-1}). To the contrary, hypothetic Na_2TeS_3-*mC*48 is significantly less favored (ΔE = 1.8 kJ mol^{-1}) than the primitive modification. Na_2TeS_3 and Na_2TeSe_3-*mP*24 are isotypic to Li_2TeS_3, whereas Na_2TeSe_3-*mC*48 crystallizes in its own structure type, which was first described by Eisenmann and Zagler. The title compounds have two common structure motifs. Trigonal TeQ_3 pyramids form layers, and the Na atoms are surrounded by a distorted octahedral environment of chalcogen atoms. Raman spectra are dominated by the vibration modes of the TeQ_3 units. The activation energies of the total conductivity of the title compounds range between 0.68 eV (Na_2TeS_3) and 1.1 eV (Na_2TeSe_3). Direct principal band gaps of 1.20 and 1.72 eV were calculated for Na_2TeSe_3 and Na_2TeS_3, respectively. The optical band gaps are in the range from 1.38 eV for Li_2TeSe_3 to 2.35 eV for Na_2TeS_3.

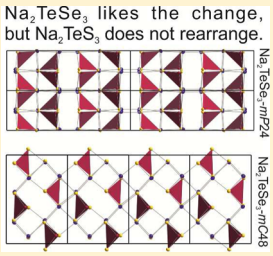

INTRODUCTION

Research on ternary chalcogenidotellurates started early in the 20th century. The first experiments on such compounds were limited on aqueous solutions. Gutbier and Flury investigated a solution of NaOH and tellurium sulfide, which was saturated with H_2S. The observed precipitate was interpreted as the monohydrate $Na_2TeS_3{\cdot}H_2O$.[1] Alternatively, $Te_2O_3(OH)NO_3$ was used to synthesize numerous anhydrates and dihydrates of ternary sulfidotellurates(IV) with other mono- and bivalent cations in several investigations by Schäfer and co-workers. They precipitated K_2TeS_3, K_3TeS_4, Rb_3TeS_4, $(NH_4)_2TeS_3$, $(NH_4)_2TeS_3{\cdot}2H_2O$, and $BaTeS_3{\cdot}2H_2O$ by passing H_2S in aqueous solutions of $Te_2O_3(OH)NO_3$ and KOH, respectively $RbOH{\cdot}2H_2O$, NH_4OH, or $Ba(OH)_2$.[2] No structure determinations were performed in the case of K_3TeS_4 and Rb_3TeS_4 to date, and therefore the nature of these two compounds is not yet clear. Further anhydrates of both thio- and selenotellurates(IV) were exclusively accessible by solid-state reactions. Jumas and co-workers obtained $BaTeS_3$ and $Ba_3Te_2S_7$ from mixtures of BaS, Te, and S, whereas Bensch and co-workers converted tellurium in a potassium polysulfide flux to K_2TeS_3.[3] Recently, Schleid and co-workers presented the heavier homologue Cs_2TeS_3.[4] Li_2TeS_3 and Li_2TeSe_3 were reported by Pfitzner and co-workers.[5b,c] Zagler and Eisenmann reported Na_2TeSe_3-*mC*48.[5a] These compounds were also obtained by solid-state reactions from the elements. In the literature, *mP*24 modifications of Na_2TeS_3 and Na_2TeSe_3 were unknown to date.

The structures of these chalcogenidotellurates(IV) are mostly well determined. $BaTeS_3$, $BaTeS_3{\cdot}2H_2O$, and $(NH_4)_2TeS_3$ crystallize in orthorhombic space groups,[2] whereas the corresponding alkali-metal compounds crystallize in the monoclinic crystal system. Their structures have layers of trigonal-pyramidal TeQ_3 units (Q = S, Se) in common. The countercations are located between these layers and are six-coordinated by the chalcogenide atoms. Li_2TeQ_3 compounds (Q = S, Se) are isotypic and crystallize in their own structure type with a coordination number of 6 for Li.[5b,c] K_2TeS_3 and Cs_2TeS_3 show some similarities in comparison to these lithium compounds. However, their crystal structures differ from each other because of the different orientations of the TeS_3 units within the layers.[3,4]

Chalcogenidotellurates(IV) containing coinage metals besides alkali-metal cations are also known. Zhang and Kanatzidis reported new two-dimensional monoclinic structure types for isostructural $RbCuTeS_3$, $KAgTeS_3$, $RbAgTeS_3$, and $CsAgTeS_3$. Monovalent Ag and Cu ions are incorporated in the TeS_3 layers via tetrahedral coordination by S, and alkali-metal ions reside between the layers.[6]

A compound with the composition "Cu_2TeS_3" has not been reported to date. However, Pfitzner and co-workers were able to create layers of this composition, which were embedded in CuX (X = Cl, I) matrixes to form the compounds

Received: September 11, 2015
Published: November 24, 2015

DOI: 10.1021/acs.inorgchem.5b02105
Inorg. Chem. 2015, 54, 11457−11464

Table 1. Crystallographic Data of Na_2TeS_3, Na_2TeSe_3-*mP*24, and Na_2TeSe_3-*mC*48

	Na_2TeS_3	Na_2TeSe_3-*mP*24	Na_2TeSe_3-*mC*48
color	yellow	red	red
M_w/(g mol^{-1})	269.76	410.46	410.46
cryst syst	monoclinic	monoclinic	monoclinic
space group	$P2_1/c$ (No. 14)	$P2_1/c$ (No. 14)	$C2/c$ (No. 15)
a/Å	5.776(1)[a]	5.990(1)[a]	21.6801(9),[a] 21.627(1)[b]
b/Å	12.202(3)[a]	12.658(3)[a]	5.9754(2),[a] 5.9730(2)[b]
c/Å	8.405(3)[a]	8.784(2)[a]	11.9736(7),[a] 11.9519(6)[b]
β/deg	92.02(2)[a]	93.51(3)[a]	121.166(6),[a] 121.228(7)[b]
V /Å^3	592.0(3)[a]	664.8(2)[a]	1326.8(2),[a] 1320.3(1)[b]
Z	4	4	8
ρ_{calc}/(g cm^{-3})	3.027	4.101	4.141,[a] 4.130[b]
temperature T/K	293	293	293,[a] 123[b]
diffractometer	STOE IPDS, graphite monochromator	STOE IPDS, graphite monochromator	Oxford Diff. Mova, graphite monochromator
λ(Mo Kα)/Å	0.71073	0.71073	0.71073
μ(Mo Kα)/mm^{-1}	6.073	20.893	21.095
abs corrn	numerical; crystal description with 7 faces; shape optimized with *X-SHAPE*[12]	numerical; crystal description with 19 faces; shape optimized with *X-SHAPE*[12]	analytical; Clark and Reid[13] crystal description optimized with *SCALE ABSPACK*[13]
2θ range/deg	$5.88 \le 2\theta \le 51$	$5.66 \le 2\theta \le 52.16$	$6.82 \le 2\theta \le 51$
hkl ranges	$-7 \le h \le 7$	$-7 \le h \le 7$	$-31 \le h \le 31$
	$-16 \le k \le 16$	$-15 \le k \le 15$	$-5 \le k \le 8$
	$-10 \le l \le 9$	$-10 \le l \le 10$	$-17 \le l \le 17$
no. of param	55	55	55
no. of reflns, R_{int}	5996, 0.0325	4729, 0.0384	6942, 0.0387
no. of indep reflns	1381	1308	2147
final R1, wR2 [$I > 2\sigma(I)$]	0.0175, 0.0463	0.0239, 0.0621	0.0352, 0.0745
final R1, wR2 (all reflns)	0.0208, 0.0451	0.0272, 0.0608	0.0326, 0.0730
GOF	1.015	0.981	1.080
largest diff peak $\Delta\rho_{max}$, hole $\Delta\rho_{min}$/(e Å^{-3})	0.557, −0.432	1.03, −0.701	1.363, −2.726

[a]Parameters refined from powder X-ray diffraction data at room temperature. [b]Parameters refined from single-crystal diffraction data at 123 K.

$CuClCu_2TeS_3$ and $(CuI)_3Cu_2TeS_3$. Therein TeS_3^{2-} units are also arranged in layers, and Cu occupies both trigonal-planar and tetrahedral sites.[7] Kanatzidis and co-workers observed the corresponding Ag-containing layers Ag_2TeS_3 in the compounds $Ag_2TeS_3{\cdot}Rb_2S_6$ and $Ag_2TeS_3{\cdot}Cs_2S_6$, in which they are separated by polysulfide chains S_6^{2-}.[8] Furthermore, pure, monoclinic Ag_2TeS_3 (space group *Cc*) was presented by Pertlik.[9] The tetrahedral coordination of Ag remains, even when 75% of Ag is replaced by Na. The resulting compound has the composition $Na_{1.5}Ag_{0.5}TeS_3$ with a 1:1 mixing of Ag and Na on one of two Ag sites.[9] A complete substitution of Ag by Na results in the title phase Na_2TeS_3, which was reported by Preitschaft.[5b] He found that Na_2TeS_3 and Na_2TeSe_3 are isotypic with Li_2TeQ_3, which crystallizes in the space group $P2_1/c$.[5b,c] However, Zagler and Eisenmann proposed a different structure type for Na_2TeSe_3 with the space group $C2/c$ in an earlier communication.[5a]

Herein, we present the first sodium thiotellurate(IV) and a new phase of Na_2TeSe_3. The structural results are interpreted by taking Raman spectroscopy, thermal analysis, and density functional theory (DFT) calculations into account. Also, the question of why two different modifications are observed for the selenide but only one for the sulfide is discussed.

■ EXPERIMENTAL SECTION

General Synthetic Procedure. All samples were synthesized and manipulated in a glovebox under an argon atmosphere. Na_2TeS_3 and Na_2TeSe_3 were synthesized from the elements Na (99%, Merck), Te (99.999%, Chempur), S (99.999%, Chempur), and Se (99.99+%, Chempur), respectively, in the stoichiometric ratio 2:1:3. The starting materials were filled in graphite crucibles, which were sealed in evacuated silica ampules. The samples of Na_2TeS_3 and Na_2TeSe_3-*mC*48 were heated up to 1170 K (1 K min^{-1}) in order to obtain well-crystalline material. After 3 h, they were slowly cooled to room temperature (0.1 K min^{-1}). Na_2TeSe_3-*mP*24 was obtained by annealing the elements at 670 K for 10 days. The lithium compounds were synthesized as described in ref 5c.

Powder X-ray Diffraction. X-ray diffraction on powdered samples was performed with a Huber diffractometer (Cu Kα_1 radiation; λ = 1.540598 Å; Ge(111) monochromator; imaging-plate camera system G670) to prove the purity of the samples. They were fixed between two mylar films (Mylar Polyester, Chemplex). A thin film of mineral oil prevented decomposition of the compounds by air. Data were collected in a 2θ range of 10−80° with a step size of 0.005°. The STOE *WINXPOW* program package was used for indexing and cell refinements.[10] The cell parameters were finally refined with *JANA2006*.[11]

Crystal Structure Determination. Data for the crystal structure determination of Na_2TeS_3 and Na_2TeSe_3-*mP*24 were obtained by single-crystal X-ray diffraction (Stoe IPDS I; graphite monochromator; Mo Kα radiation; λ = 0.71073 Å). The crystals were fixed on top of glass fibers and measured in sealed glass capillaries at room temperature. Absorption was corrected numerically by *X-RED* after optimization of the crystal-shape description with *X-SHAPE*.[12] A single crystal of Na_2TeSe_3-*mC*48 was measured additionally at low temperatures on an Oxford CCD diffractometer equipped with a MOVA microsource (Mo Kα radiation; λ = 0.71073 Å). A Cryojet unit maintained a sample temperature of 123 K. The crystal was fixed on a microloop in mineral oil. The crystal-shape description was optimized with SCALE3 ABSPACK, and an analytical absorption correction according to Clark and Reid was applied.[13] The structure models of

DOI: 10.1021/acs.inorgchem.5b02105
Inorg. Chem. 2015, 54, 11457−11464

the title compounds were solved with *SHELXS97* by direct methods and refined on the basis of full-matrix least squares with *SHELXL97*.[14]

Differential Thermal Analysis (DTA). The measurements were performed with a Setaram DTA-TG 92-16.18 with Al_2O_3 as the standard. Small amounts of the title compounds were sealed in evacuated quartz tubes (1.5 mm in diameter). DTA data were recorded up to 1073 K with heating and cooling rates of 10 K min^{-1}.

Raman Spectroscopy. Raman spectra were recorded with a Varian FTS 7000e spectrometer with a Nd:YAG laser (excitation wavelength λ = 1064 Å), a Varian FT-Raman module, and a liquid-nitrogen-cooled germanium detector. Data were collected in back-scattering mode. The powder samples were sealed in Duran glass capillaries (external diameter 1.5 mm).

Theoretical Calculations. All quantum-chemical calculations were performed within the DFT-generalized gradient approximation (GGA) functional Perdew−Burke−Ernzerhof.[15] Full geometry optimizations were performed with the projector-augmented-wave[16] approach and the conjugant gradient algorithm, as implemented in the code of the Vienna ab initio simulation package (*VASP 4.6*);[16] see also ref 17. Convergence is considered at differences in the total energy of less than 10^{-5} eV and maximum Hellmann−Feynman forces of 10^{-4} eV $Å^{-1}$. Density of states (DOS) and band-structure calculations were executed with the scalar relativistic full-potential local orbital scheme FPLO14, which optimizes valence functions at each self-consistent-field step.[18a,b] The calculations were converged to 4 × 4 × 4 *k*-point meshes.

UV/Vis Spectroscopy. For the optical-band-gap determination, the samples were diluted with $BaSO_4$ (pure Ph. Eur. AppliChem) and measured with a Bruins Omega 20 spectrometer in remission mode with a resolution of 1 nm. The wavelength of the emitted light ranged between 380 and 1100 nm. The instrument was operated by the software *OMEGA Analyzer*.[19a] 100% remission was defined for the pure standard $BaSO_4$. The remission was converted to absorption using the Kubelka−Munk function.[19b,c] The optical band gap was assumed as the intersection of linear extrapolations of the baseline and absorption edge.

Impedance Spectroscopy. Complex impedance spectra were recorded with an IM6 analyzer (Zahner Electrik, Meßtechnik, Germany) under an argon atmosphere. Therefore, finely ground powders were pressed to pellets with at least 90% of the crystallographic density. The pellets were contacted to Au electrodes and transferred to a homemade measuring cell. Spectra were recorded in the range from 1 Hz to 1 MHz. The *Thales Flink* software was used for operation and data evaluation.[20] A detailed description of the setup is given in ref 21.

■ RESULTS AND DISCUSSION

Crystal Structure of Na_2TeS_3. Na_2TeS_3 crystallizes in the space group $P2_1/c$ with the lattice parameters a = 5.776(1) Å, b = 12.202(3) Å, c = 8.405(3) Å, β = 92.02(2)°, and V = 592.0(3) $Å^3$ (Z = 4). Crystallographic details are listed in Table 1. Na_2TeS_3 is isotypic with Li_2TeS_3. For a better comparison, we chose the same crystallographic settings in Table 2 as those in ref 5a. All atoms reside on the Wyckoff position 4e. The sulfide ion sites S1, S2, and S3 constitute a distorted cubic-close-packed anionic framework with a total of 12 octahedral voids per unit cell. Therein, Te^{IV} cations occupy one-third of crystallographic equivalent octahedral sites, with a strong 3 + 3 splitting of the distances d(Te−S).

Te atoms have three S atoms in a distance of about 2.4 Å and three additional S atoms in larger distances of about 3.5 Å. This is due to the predominantly covalent bonding character of the Te−S bonds. The 3 + 3 coordination of Te is shown in Figure 1a. The three short distances d(Te−S) in these isolated trigonal

Table 2. Atomic Coordinates and Equivalent Isotropic Displacement Parameters U_{eq}/$Å^2$ for Na_2TeS_3 at Room Temperature

atom[a]	x	y	z	U_{eq}
Na1	0.7402(2)	0.76002(9)	0.1240(2)	0.0294(2)
Na2	0.2458(2)	0.91664(8)	0.3641(2)	0.0273(2)
Te	0.70928(2)	0.08813(2)	0.18461(2)	0.01804(7)
S1	0.3051(1)	0.09304(5)	0.13899(9)	0.0219(1)
S2	0.7612(1)	0.23360(5)	0.36856(8)	0.0216(1)
S3	0.7482(1)	0.93561(5)	0.35327(8)	0.0227(1)

[a]All atoms are located on the Wyckoff site 4e.

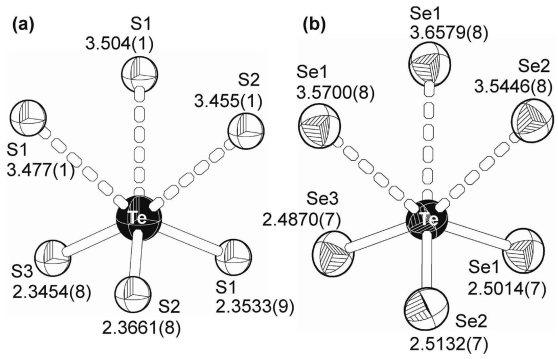

Figure 1. 3 + 3 coordination of Te by the chalcogenide anions in (a) Na_2TeS_3 and (b) Na_2TeSe_3-*mP*24 and the interatomic distances d(Te−S) and d(Te−Se) given in angstroms.

TeS_3 pyramids range from 2.345 to 2.366 Å, as was already observed for similar compounds. For example, an average value of $\bar{d}$(Te−S) = 2.367 Å was reported for Li_2TeS_3 and $\bar{d}$(Te−S) = 2.350 Å for K_2TeS_3.[3,5c] The smallest distances d(Te−S) in this series of alkali-metal compounds were recently found in Cs_2TeS_3 (2.312−2.349 Å).[3]

The size of the alkali metal M has only a minor influence on the distance d(Te−S). The values slightly decrease with increasing radius and increasing electropositivity of M. An opposite trend is found for the angles S−Te−S in this series of compounds. They become larger for the heavier alkali-metal thiotellurates. Thus, they range between 100.9° and 101.1° in Na_2TeS_3. They are larger than those in Li_2TeS_3 (99.2−100.5°) and smaller than those in K_2TeS_3 (102.1−103.1°) and Cs_2TeS_3 (102.7−106.9°).[3−5]

The Na cations occupy two-thirds of the distorted octahedral voids in the sulfide substructure. Figure 2 shows such NaS_6 motifs for the two different sites Na1 and Na2. It is remarkable that the distance d(Na1−S3) = 3.299 Å deviates significantly from all other distances d(Na−S), which are considerably smaller than 3 Å. This specific distance is about 15% longer than the sum of the ionic radii (2.86 Å).[22] Therefore, this surrounding is better described as a 5 + 1 coordination. In contrast, the distances d(Na2−S) are more or less in the range of the sum of the ionic radii. All six values for d(Na2−S) range from 2.882 to 2.981(2) Å. This effect is even more pronounced in the case of the isotypic compound Li_2TeS_3.[5c]

This structural peculiarity is also observed in chalcogenidotellurates, which are not isotypic to Na_2TeS_3. In K_2TeS_3, for example, one longer distance d(K−S) = 3.536 Å and an average value of $\bar{d}$(K−S) = 3.22 Å for the other distances are observed.[3] The angles S−Na−S are almost unaffected by this one elongated interatomic distance. They range from 78.0 to 177.6° for S−Na1−S and from 76.4 to 170.2° for S−Na2−S.

DOI: 10.1021/acs.inorgchem.5b02105
Inorg. Chem. 2015, 54, 11457−11464

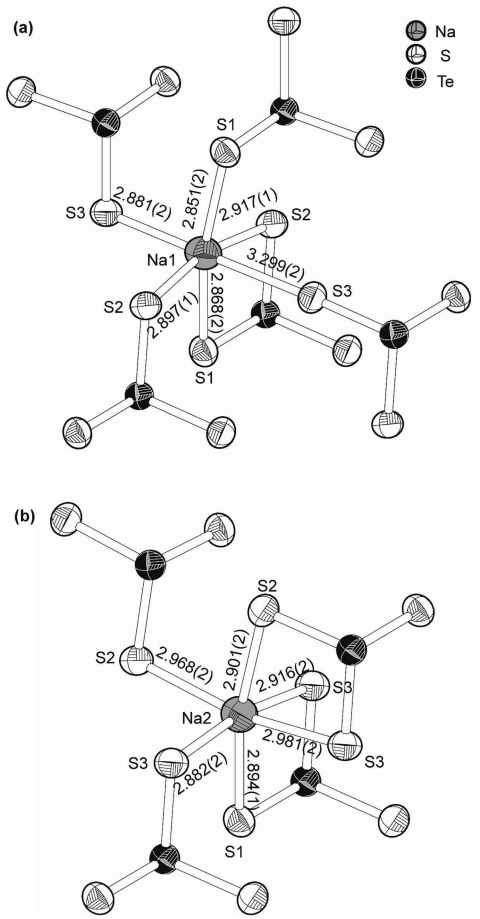

Figure 2. Different coordination of the sites (a) Na1 and (b) Na2 by the trigonal TeS_3 pyramids, which act as mono- or bidentate ligands.

Table S2 summarizes the corresponding data. Apart from these distortions, both Na sites show also a difference with respect to the coordination mode of the TeS_3 units; see Figure 2. $Na1S_6$ octahedra are connected to four monodentate TeS_3 ligands and one bidentate TeS_3 ligand. $Na2S_6$ octahedra are connected to two monodentate and two bidentate TeS_3 ligands. Multidentate TeS_3 ligands are also known from other structure types like, e.g., Cs_2TeS_3.[4]

Crystal Structure of Na_2TeSe_3-*mP*24. The red compound Na_2TeSe_3-*mP*24 is isotypic to Na_2TeS_3 and has the lattice parameters a = 5.990(1) Å, b = 12.658(3) Å, c = 8.784(2) Å, β = 93.51(3)°, and V = 664.8(2) Å^3 (Z = 4), which were refined from powder X-ray diffraction data (Table 3).

Table 3. Atomic Coordinates and Equivalent Isotropic Displacement Parameters U_{eq}/Å^2 for Na_2TeSe_3-*mP*24 at Room Temperature

atom[a]	x	y	z	U_{eq}
Na1	0.7389(3)	0.7616(2)	0.1296(2)	0.0382(4)
Na2	0.2461(3)	0.9167(1)	0.3627(2)	0.0362(4)
Te	0.70263(4)	0.08924(2)	0.18948(3)	0.0260(1)
Se1	0.28807(7)	0.09232(2)	0.13406(5)	0.0302(1)
Se2	0.76189(7)	0.23828(3)	0.37661(5)	0.0293(1)
Se3	0.74859(7)	0.93291(4)	0.36001(5)	0.0307(1)

[a]All atoms are positioned on the Wyckoff site 4e.

The distances d(Te−Se) suggest the motif of isolated $TeSe_3$ units. Three short distances are between 2.4869 and 2.5131 Å, whereas the distances to the second-nearest neighbors range from 3.545 to 3.658 Å. A comparison of these direct contacts and the mean distances to next-nearest neighbors $\bar{d}_{sec}$(Te−Se) in the compounds Li_2TeSe_3 (2.513 Å) or K_2TeSe_3 (2.491 Å) and the mean distances $\bar{d}_{sec}$(Te−Se) in M_2TeSe_3 show a reduction of d with increasing size and electropositivity of the cation.[3,5]

The distortion of the octahedron $Na2Se_6$ is less pronounced than that of the octahedron $Na1Se_6$. All values of d(Na2−Se) range between 2.986 and 3.090 Å. For d(Na1−Se), five values are between 2.960 and 3.011 Å. The shorter bond lengths are comparable to those in Na_3SbSe_3 (2.992−3.218 Å).[23] The largest value in Na_2TeSe_3-*mP*24 is observed for d(Na1−Se3) = 3.419 Å. Compounds with primary coordination spheres with d(Na−Se) > 3.4 Å are quite rare. Ohtani and co-workers reported similar values (3.437 and 3.500 Å) for the compounds $NaTM_5Se_8$ (TM = Ti, Cr).[24] Details of the three-dimensional linkage of the building blocks are the same as those for Na_2TeS_3-*mP*24 vide supra.

Crystal Structure of Na_2TeSe_3-*mC*48. The crystal structure of Na_2TeSe_3-*mC*48 was first determined by Zagler and Eisenmann.[5a] However, we herein present the results of a new structure determination at low temperature, which confirms their results. In addition, structural correlations between both phases of Na_2TeSe_3 and their thermal transformation are discussed. Na_2TeSe_3-*mC*48 crystallizes in the space group $C2/c$ with a = 21.627(1) Å, b = 5.9730(2) Å, c = 11.9519(6) Å, β = 121.228(7)°, and V = 1320.3(1) Å^3 (Z = 8) (data collected at 123 K). The cell parameters of Na_2TeSe_3-*mC*48 were refined from powder X-ray diffraction data with *JANA2006* to a = 21.6801(9) Å, b = 5.9730(2) Å, c = 11.9519(6) Å, β = 121.228(7)°, and V = 1326.8(2) Å^3 at room temperature. They are in good agreement with the data of Zagler and Eisenmann.[5a] For a better comparison, we chose their setup of atomic parameters (see Table 4). Both

Table 4. Atomic Coordinates and Equivalent Isotropic Displacement Parameters U_{eq}/Å^2 for Na_2TeSe_3-*mC*48 at Room Temperature

atom[a]	x	y	z	U_{eq}
Na1	0.75184(9)	0.0108(3)	0.1246(2)	0.0164(4)
Na2	0.9274(1)	0.4686(2)	0.8076(2)	0.0178(4)
Te	0.89304(2)	0.04964(4)	0.49288(2)	0.01134(8)
Se1	0.91021(2)	0.46339(6)	0.54187(4)	0.0130(1)
Se2	0.91422(2)	0.03137(6)	0.30581(4)	0.0134(1)
Se3	0.75919(2)	0.00938(6)	0.38250(4)	0.0128(1)

[a]All atoms are positioned on the Wyckoff site 8f.

modifications of Na_2TeSe_3 have the already mentioned cubic-closed-packed framework of selenide anions in common. The difference between the structures is due to the way how the octahedral voids are occupied by sodium and tellurium. The two different ordering schemes of cations are shown in Figure 3. Because the unit cell volume of Na_2TeSe_3-*mC*48 is twice that of Na_2TeSe_3-*mP*24, the cell has 24 occupied octahedral sites.

The crystal structure of Na_2TeSe_3-*mC*48 consists of the same basic building units as the second modification Na_2TeSe_3-*mP*24, trigonal-pyramidal $TeSe_3$ units and two octahedrally coordinated Na sites (Figure 4). Again, one of these $NaSe_6$ octahedra shows one pronounced long distance d(Na2−Se) =

DOI: 10.1021/acs.inorgchem.5b02105
Inorg. Chem. 2015, 54, 11457−11464

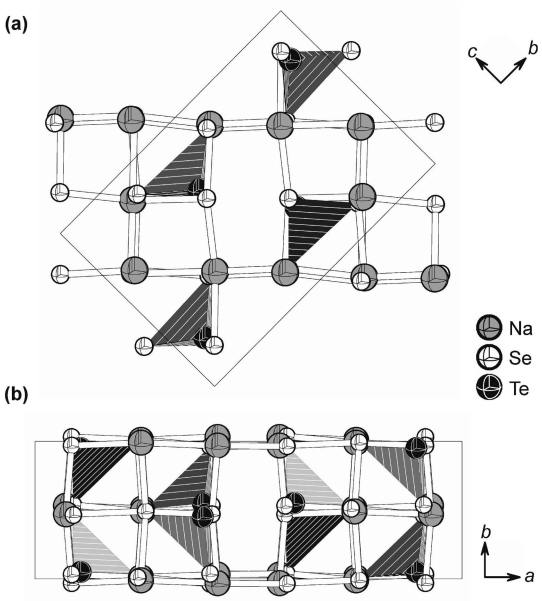

Figure 3. Ordering schemes of Te and Na in the cubic-closest-packed framework of Se anions in the case of (a) Na_2TeSe_3-*mP*24 and (b) Na_2TeSe_3-*mC*48. The $TeSe_3$ pyramids are illustrated in dark gray.

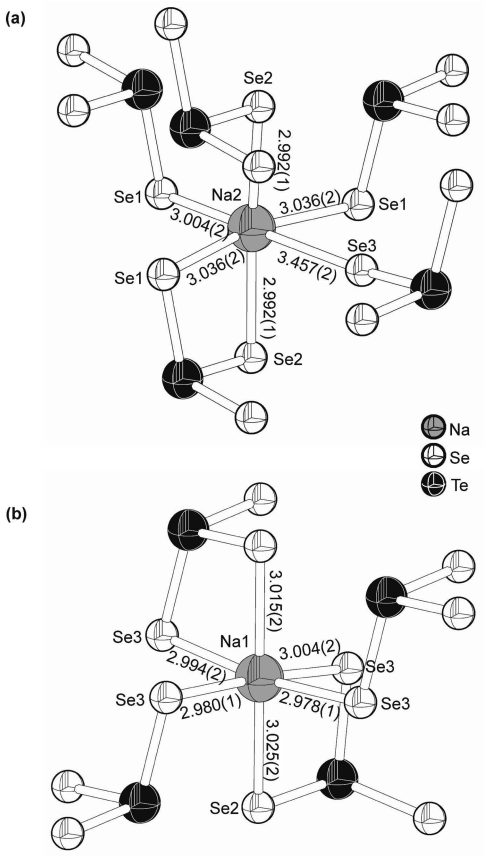

Figure 4. Trigonal $TeSe_3$ pyramids act as mono- or bidentate ligands in Na_2TeSe_3-*mC*48 similar to that in Na_2TeSe_3-*mP*24.

3.457(2) Å. It is connected to four monodentate $TeSe_3$ ligands and one bidentate $TeSe_3$ ligand, whereas the less distorted octahedron is connected to two monodentate and two bidentate $TeSe_3$ ligands. The interatomic distances are generally almost identical for both phases of Na_2TeSe_3 (compare Tables S4 and S6).

Raman Spectroscopy. To date, vibration modes of the TeS_3 and $TeSe_3$ units were observed only for a few compounds. In the case of thiotellurates(IV), for example, the Raman shifts ν(Te−S) for Cs_2TeS_3 (392, 370, and 192 cm^{-1}),[4] Tl_2TeS_3 (338, 309, 180, and 154 cm^{-1}),[25] $CuClCu_2TeS_3$ (359, 336, 274, 247, and 155 cm^{-1}), and $(CuI)_3Cu_2TeS_3$ (371, 360, 328, and 108 cm^{-1}) were reported.[7] They resemble each other in the number of detected signals and their intensity ratio because of their similar local symmetry. An ideal C_{3v} symmetry of the TeS_3 units was observed in $CuClCu_2TeS_3$.[7] A crystallographic symmetry reduction resulting in a structural distortion of the TeS_3 pyramids leads to the point groups C_s (as reported for Tl_2TeS_3) and C_1 like in $(CuI)_3Cu_2TeS_3$. The latter holds also for the title compounds.

For Na_2TeS_3, we observed signals at 367, 353, 341, and 159 cm^{-1} (see Figure 5). This corresponds to the values reported

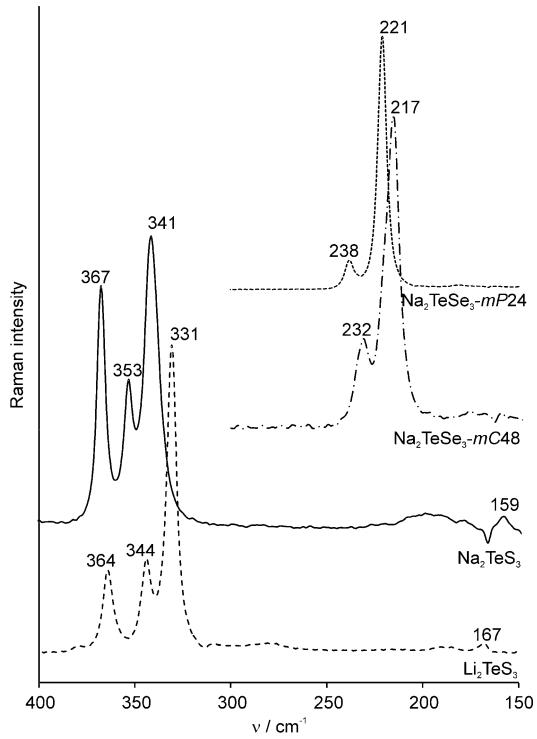

Figure 5. Raman spectra of Li_2TeS_3 (broken line), Na_2TeS_3 (solid line), Na_2TeSe_3-*mP*24 (dotted line), and Na_2TeSe_3-*mC*48 (broken-dotted line).

for $(CuI)_3Cu_2TeS_3$. The different Raman shifts can be explained by the varying values of d_{sec}(Te−S) in these compounds. The longer d_{sec}(Te−S), the stronger are the three short bonds and the higher are the Raman resonances. For this reason, the Raman spectra of the isotypic compound Li_2TeS_3 (broken line) differs slightly from that of Na_2TeS_3. The signals are red-shifted to values of 364, 344, 331, and 167 cm^{-1}. The mean distances to the next-nearest neighbors $\bar{d}_{sec}$(Te−S) in Na_2TeS_3 are significantly longer than those in Li_2TeS_3, whereas in both compounds, the three short distances d(Te−S) are more or less identical. The average of $\bar{d}_{sec}$(Te−S) in Li_2TeS_3 is 3.200 Å, and $\bar{d}$ = 3.479 Å in Na_2TeS_3. This is attributed to an increasing ionicity of the compound due to substitution of Li by Na. In the case of K_2TeS_3, a mean distance of $\bar{d}_{sec}$(Te−S) =

DOI: 10.1021/acs.inorgchem.5b02105
Inorg. Chem. 2015, 54, 11457−11464

3.928 Å is observed. However, no Raman shifts were reported for this compound, but IR studies were published by Zhang and Kanatzidis. They reported the strongest far-IR shifts at 371, 347, 210, and 190 cm^{-1}.[6] Although the selection rules differ for IR and Raman spectroscopy, the shifts in these spectra may be taken for comparison. For the heaviest homologue Cs_2TeS_3, Schleid and co-workers observed the Te−S Raman modes at 392, 370, 192, and 176 cm^{-1}.[4] Considering $\bar{d}_{sec}$(Te−S) is longer than 4 Å in Cs_2TeS_3, these shifts confirm the described trend. Kysliak and Beck observed Raman modes between 260 and 218 cm^{-1} for $[Zn(NH_3)_4]TeSe_3$.[26] The spectra of the *mP*24 and *mC*48 modifcations of Na_2TeSe_3 show signals from 238 to 217 cm^{-1}; see Figure 5. The surroundings of Te in these modifications are almost equal, which explains the similarity of the spectra.

Theoretical Calculations. At first, DFT calculations focused on the polymorphism of Na_2TeSe_3 and the attempt to understand why no phase transition is observed for Na_2TeS_3. Total energy calculations were performed on completely optimized structures to elucidate the relative stabilities of both polymorphs (Figure 6). In addition, a hypothetic,

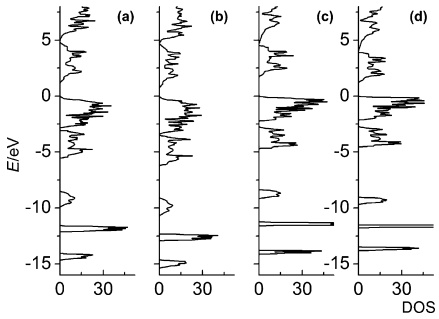

Figure 6. Calculated total DOS of the isotypic compounds (a) Li_2TeS_3, (b) Li_2TeSe_3, (c) Na_2TeS_3, and (d) Na_2TeSe_3-*mP*24.

isostructural modification Na_2TeS_3-*mC*48 was estimated. Predicted cell volumes are overestimated compared to the experiments, as is known for GGA methods, but the deviations are similar for both modifications. A difference in energy of ΔE = 1.8 kJ mol^{-1} is calculated for hypothetic Na_2TeS_3-*mC*48 compared to the modification *mP*24. This difference is smaller by 1 order of magnitude for the *mP*24 and *mC*48 modifications of Na_2TeSe_3 (ΔE = 0.18 kJ mol^{-1}). Such differences were identified as decisive whether structures are formed under equilibrium conditions in recent systematic investigations on the phase stabilities.[17] From the present calculations, Na_2TeS_3-*mC*48 is predicted as less stable on the potential energy surface (0 K). However, it might be accessible by nonequilibrium methods. Its predicted crystal structure shows the same features as those of Na_2TeSe_3-*mC*48. A detailed analysis is, however, beyond the scope of the present paper.

The calculated electronic band structures of the title compounds are compared to Li_2TeQ_3 (Q = S, Se). One can find a systematic trend in the change of the optical band gaps with the composition of the *mP*24 modifications (Table 5, Figure 7, and Figure S2). The calculated band gap (DFT-GGA) decreases in accordance with the experimentally found colors when S is replaced by Se from 1.71 eV (Na_2TeS_3) to 1.18 eV (Na_2TeSe_3). When Na is replaced by Li, even smaller band gaps of 1.20 and 0.73 eV are calculated for Li_2TeS_3 and Li_2TeSe_3, respectively. Interestingly, the predicted gap slightly increases from the *mP*24 and *mC*48 modifications (1.20 eV),

Table 5. Calculated Electronic Band Gaps ΔE^{calc} of M_2TeQ_3 from DFT-GGA in Comparison to the Experimentally Determined Optical Band Gap ΔE^{exp}_{opt}

	ΔE^{calc}/eV	ΔE^{exp}_{opt}/eV
Li_2TeS_3	1.197	1.95
Li_2TeSe_3	0.727	1.38
Na_2TeS_3-*mP*24	1.714	2.35
Na_2TeS_3-*mC*48[a]	1.468	
Na_2TeSe_3-*mP*24	1.179	1.87
Na_2TeSe_3-*mC*48	1.203	1.95

[a]Hypothetical modification.

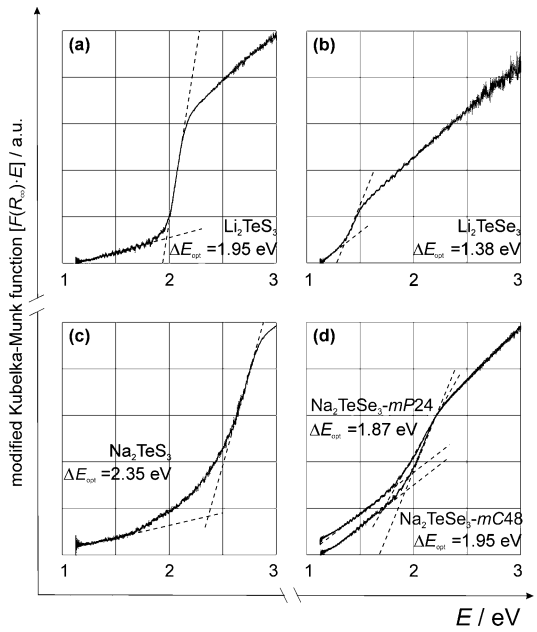

Figure 7. Optical absorption spectra of M_2TeQ_3 (M = Li, Na; Q = S, Se). The spectra of both modifications of Na_2TeSe_3 are displayed in part d and are almost identical.

whereas it is significantly lowered for the hypothetical Na_2TeS_3-*mC*48 (1.47 eV). The band-structure plots in Figure S2 of the title compounds indicate direct band gaps (see Figure S2). The underestimation of the absolute values is a well-known effect of DFT functionals.

UV/Vis Spectroscopy. We carried out UV/vis spectroscopic measurements on Li_2TeQ_3, Na_2TeS_3, and both modifications of Na_2TeSe_3 in order to verify the results of DFT calculations; see Figure 7. The detected optical band gaps range between 1.38 and 2.35 eV. The smallest optical band gap was measured for dark-gray Li_2TeSe_3 and the largest band gap for yellow Na_2TeS_3. The other samples show band gaps in the medium range of Li_2TeS_3 (1.95 eV), Na_2TeSe_3-*mC*48 (1.95 eV), and Na_2TeSe_3-*mP*24 (1.87 eV).

The optical band gaps of tellurates(IV) under discussion increase with increasing ionicity of the alkali metals and chalcogens. The band gap of Li_2TeS_3 is 0.40 eV smaller than that of Na_2TeS_3. Likewise, the alkali cation influences the band gap of the selenide compounds: The band gap of Li_2TeSe_3 is 0.49 eV smaller than the one of Na_2TeSe_3. The influence of the chalcogenide on the optical properties is slightly stronger. Thus, the band gap of Li_2TeSe_3 is 0.57 eV smaller than that of Li_2TeS_3. A similar relationship is observed for the sodium compounds. The optical band gap of Na_2TeSe_3 is 0.48 eV

DOI: 10.1021/acs.inorgchem.5b02105
Inorg. Chem. 2015, 54, 11457−11464

smaller than that of Na_2TeS_3. Whereas the ionicity of the alkali cation and chalcogenide anion increases the band gaps, the structural differences between the *mP*24 and *mC*48 modifications have no significant influence on the optical properties. Almost equal band gaps are found for Na_2TeSe_3-*mP*24 (1.87 eV) and Na_2TeSe_3-*mC*48 (1.95 eV). The optical band gaps of M_2TeQ_3 (M = Li, Na; Q = S, Se) are significantly higher than those of Ag_2TeS_3 (0.35 eV), whereas the absorption behavior of Na_2TeSe_3 and Li_2TeS_3 is similar to that of (Ag_2TeS_3) Rb_2S_6 and (Ag_2TeS_3) Cs_2S_6 (2.0 eV).[8]

Impedance Spectroscopy. The temperature-dependent total conductivities of Na_2TeS_3 and the isotypic modification of Na_2TeSe_3-*mP*24 were analyzed by impedance spectroscopy. The Arrhenius plots of these compounds and the isotypic Li compounds in Figure 8 show a linear dependence of the logarithm of the specific conductivity σ_{spez} and the reciprocal temperature. The conductivities increase with increasing temperature.

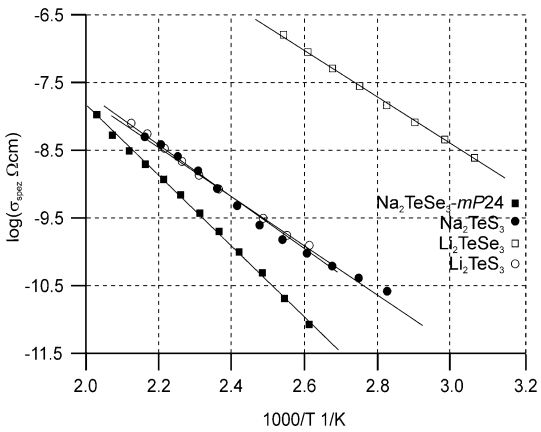

Figure 8. Arrhenius plot of the total conductivities of isotypic M_2TeQ_3 (M = Li, Na; Q = S, Se).

In the case of Na_2TeS_3, the conductivity ranges between 1×10^{-10} $(\Omega\ cm)^{-1}$ at 370 K and 4.1×10^{-9} $(\Omega\ cm)^{-1}$ at 470 K. Similar values are observed for Na_2TeSe_3 [$\sigma_{spez} = 8.7 \times 10^{-12}$ $(\Omega\ cm)^{-1}$ at 370 K and $\sigma_{spez} = 3.1 \times 10^{-9}$ $(\Omega\ cm)^{-1}$ at 470 K]. The different ionicity of the chalcogens has only a very weak influence on the total conductivity. Larger differences were observed in the case of the lithium compounds. At 470 K, Li_2TeS_3 has a lower conductivity [2.5×10^{-8} $(\Omega\ cm)^{-1}$] than Li_2TeSe_3 [4.5×10^{-6} $(\Omega\ cm)^{-1}$].[4] Because the Nyquist plots of both sodium compounds do not show the typical linear spike at low frequencies, ionic contributions to the total conductivity can be regarded as quite small for Na_2TeQ_3. However, especially in the case of Na_2TeS_3, a certain ionic contribution to the total conductivity can be assumed, and therefore no clear trends can be expected for the activation energies from conductivity measurements. The activation energy for Na_2TeS_3 (0.68 eV) was significantly smaller than that for Na_2TeSe_3 (1.1 eV) and resembles the values for Li_2TeS_3 (0.71 eV) and Li_2TeSe_3 (0.68 eV).

Thermal Analysis. Na_2TeS_3 showed its melting point at 914 K (onset temperature). In the case of Na_2TeSe_3, a heating cycle was measured for both modifications. Na_2TeSe_3-*mP*24 melts at 748 K, whereas the melting point of Na_2TeSe_3-*mC*48 is observed at slightly higher temperature (766 K). However, this difference can be regarded as affected by the heating rate; i.e., one should expect a phase transformation of the low-temperature form to the high-temperature form and then an identical melting point.

CONCLUSION

We present the crystal structure of Na_2TeS_3. It is the first reported compound in the ternary phase system Na−Te−S. It is isotypic with Li_2TeQ_3 (Q = S, Se). No phase transition was observed for Na_2TeS_3. This is contrary to Na_2TeSe_3. So far, only the *mC*48 modification has been reported. Herein, we show the crystal structure of the second modification Na_2TSe_3-*mP*24, which is also isotypic with Li_2TeQ_3. The formation can be controlled by the reaction temperature, heating time, and cooling rates. The lattice energies for both modifications differ only slightly in the case of Na_2TeSe_3. For Na_2TeS_3, the calculated lattice energy of a hypothetic Na_2TeS_3-*mP*24 is significantly higher than that for Na_2TeS_3-*mC*48.

The structural differences between the *mP*24 and *mC*48 modifications of Na_2TeSe_3 hardly influence the optical band gap. They range between 1.87 eV (Na_2TeSe_3-*mP*24) and 1.95 eV (Na_2TeSe_3-*mC*48). On the other hand, Na_2TeS_3 has a larger optical band gap (2.35 eV) because of the higher iconicity of sulfur. However, the total conductivities of Na_2TeS_3 and Na_2TeSe_3 are not influenced by the differences in their iconicity. They range from 8.7×10^{-12} $(\Omega\ cm)^{-1}$ at 370 K and to 3×10^{-9} $(\Omega\ cm)^{-1}$ at 470 K.

ASSOCIATED CONTENT

Supporting Information

The Supporting Information is available free of charge on the ACS Publications website at DOI: 10.1021/acs.inorgchem.5b02105. Further details of the crystal structure investigations are available from Fachinformationszentrum (FIZ) Karlsruhe, 76344 Eggenstein-Leopoldshafen, Germany (fax + 49-7247-808-666; e-mail crysdata@fiz-karlsruhe.de) upon quoting the depository number.

Tables of the anisotropic displacement parameters U_{ij} (Tables S1, S3, and S5) of the selected interatomic distances and angles of the title compounds (Tables S2, S4, and S6), powder X-ray diffraction patterns (Figure S1), and plots of the electronic structures of M_2TeQ_3 (M = Li, Na; Q = S, Se; Figure S2) (PDF)
CSD 430311 (Na_2TeS_3) (CIF)
CSD 430313 (Na_2TeSe_3-*mP*24) (CIF)
CSD 430312 (Na_2TeSe_3-*mC*48) (CIF)

AUTHOR INFORMATION

Corresponding Author

*E-mail: arno.pfitzner@chemie.uni-regensburg.de.

Notes

The authors declare no competing financial interest.

ACKNOWLEDGMENTS

We thank Ulrike Schiessl for performing thermal analyses and Daniel Friedrich for supporting the UV/vis measurements.

REFERENCES

(1) Gutbier, A.; Flury, F. *Z. Anorg. Allg. Chem.* **1902**, *32*, 272−291.
(2) Eisenmann, B.; Katzer, H.; Schäfer, H.; Weiss, A. *Z. Naturforsch., B: J. Chem. Sci.* **1969**, *24*, 456−457. Roth, P.; Schäfer, H.; Weiss, A. *Z. Naturforsch., B: J. Chem. Sci.* **1971**, *26*, 371−372. Gerl, H.; Eisenmann, B.; Roth, P.; Schäfer, H. *Z. Anorg. Allg. Chem.* **1974**, *407*, 135−143.

DOI: 10.1021/acs.inorgchem.5b02105
Inorg. Chem. 2015, 54, 11457−11464

(3) Jumas, J.-C.; Ribes, M.; Maurin, M.; Philippot, E. *Acta Crystallogr., Sect. B: Struct. Crystallogr. Cryst. Chem.* **1976**, *32*, 444−448. Jumas, J.-C.; Maurin, M.; Philippot, E. *C. R. Acad. Sci., Ser. C* **1975**, *281*, 523−526. Rumpf, C.; Näther, C.; Bensch, W. *Acta Crystallogr., Sect. C: Cryst. Struct. Commun.* **1999**, *55*, 1046−1047.
(4) Babo, J.-M.; Wolff, K.; Schleid, T. *Z. Anorg. Allg. Chem.* **2013**, *639*, 2875−2881.
(5) (a) Zagler, R.; Eisenmann, B. *Z. Kristallogr. - Cryst. Mater.* **1988**, *183*, 193−200. (b) Preitschaft, C. Ph.D. Thesis, Universität Regensburg, Regensburg, Germany, 2005. (c) Preitschaft, C.; Zabel, M.; Pfitzner, A. *Z. Anorg. Allg. Chem.* **2005**, *631*, 1227−1232.
(6) Zhang, X.; Kanatzidis, G. M. *J. Am. Chem. Soc.* **1994**, *116*, 1890−1898.
(7) Pfitzner, A. *Inorg. Chem.* **1998**, *37*, 5164−5167. Pfitzner, A.; Reiser, S.; Nilges, T.; Kockelmann, W. *J. Solid State Chem.* **1999**, *147*, 170−176. Pfitzner, A.; Zimmerer, S. *Angew. Chem., Int. Ed. Engl.* **1997**, *36*, 982−984.
(8) Nguyen, S. L.; Jang, J. I.; Ketterson, J. B.; Kanatzidis, M. G. *Inorg. Chem.* **2010**, *49*, 9098−9100.
(9) Pertlik, F. *Monatsh. Chem.* **1997**, *128*, 157−163.
(10) *WINXPOW*, version 3.2.2.0; Stoe & Cie: Darmstadt, Germany, 2014.
(11) Petricek, V.; Dusek, M.; Palatinus, L. *Z. Kristallogr. - Cryst. Mater.* **2014**, *229*, 345−352.
(12) *X-SHAPE*, Stoe & Cie: Darmstadt, Germany, 1996. *X-RED*; Stoe & Cie: Darmstadt, Germany, 1996.
(13) *SCALE3 ABSPACK, CrysAlis RED software*, version 171.37.31; Oxford Diffraction Ltd.: Oxford, U.K., 2014. Clark, R. C.; Reid, J. S. *Acta Crystallogr., Sect. A: Found. Crystallogr.* **1995**, *51*, 887−897.
(14) Sheldrick, G. M. *SHELXS97, Program for Crystal Structure Solution*; Universität Göttingen: Göttingen, Germany, 1997. Sheldrick, G. M. *SHELXL97, Program for Crystal Structure Refinement*; Universität Göttingen: Göttingen, Germany, 1997.
(15) Perdew, J. P.; Burke, K.; Ernzerhof, M. *Phys. Rev. Lett.* **1996**, *77*, 3865−3868. Perdew, J. P.; Burke, K.; Ernzerhof, M. *Phys. Rev. Lett.* **1997**, *78*, 1396.
(16) Kresse, G. *J. Non-Cryst. Solids* **1995**, *192-193*, 222−229. Kresse, G.; Hafner, J. *Phys. Rev. B: Condens. Matter Mater. Phys.* **1994**, *49*, 14251−14269. Kresse, G.; Furthmüller, J. *Comput. Mater. Sci.* **1996**, *6*, 15−50. Kresse, G.; Furthmüller, J. *Phys. Rev. B: Condens. Matter Mater. Phys.* **1996**, *54*, 11169−11186. Kresse, G.; Joubert, D. *Phys. Rev. B: Condens. Matter Mater. Phys.* **1999**, *59*, 1758−1775.
(17) Bachhuber, F.; Rothballer, J.; Söhnel, T.; Weihrich, R. *Comput. Mater. Sci.* **2014**, *89*, 114−121. Bachhuber, F.; Rothballer, J.; Söhnel, T.; Weihrich. *J. Chem. Phys.* **2013**, *139*, 214705. Rothballer, J.; Bachhuber, F.; Rommel, S. M.; Söhnel, T.; Weihrich, R. *RSC Adv.* **2014**, *4*, 42183−42189.
(18) (a) Köpernik, K.; Eschrig, H. *Phys. Rev. B: Condens. Matter Mater. Phys.* **1999**, *59*, 1743−1757. (b) Opahle, K. K. I.; Eschrig, H.; Köpernik, K. *Phys. Rev. B: Condens. Matter Mater. Phys.* **1999**, *60*, 14035−14041.
(19) (a) *OMEGA Analyzer*, version 5.5.0.0; Bruin Instruments: Puchheim, Germany, 2006. (b) Kubelka, F.; Munk, P. Z. *Techn. Physik* **1931**, *12*, 593−601. (c) Kubelka, F.; Munk, P. *J. Opt. Soc. Am.* **1948**, *38*, 448.
(20) *Thales Flink*, version Z.2.27; Zahner Meßtechnik GmbH & Co. KG: Kronach, Germany, 2014.
(21) Freudenthaler, E.; Pfitzner, A.; Sinclair, D. C. *Mater. Res. Bull.* **1996**, *31*, 171−176.
(22) Shannon, R. D. *Acta Crystallogr., Sect. A: Cryst. Phys., Diffr., Theor. Gen. Crystallogr.* **1976**, *32*, 751−767.
(23) Pompe, C.; Pfitzner, A. *Z. Anorg. Allg. Chem.* **2012**, *638*, 2158−2162.
(24) Ohtani, T.; Sano, Y.; Kodama, K.; Onoue, S.; Nishihara, H. *Mater. Res. Bull.* **1993**, *28*, 501−508.
(25) Rieger, F.; Mudring, A.-V. *Chem. Mater.* **2007**, *19*, 221−228.
(26) Kysliak, O.; Beck, J. *Eur. J. Inorg. Chem.* **2013**, *2013*, 124−133.

■ NOTE ADDED AFTER ASAP PUBLICATION

This paper was published on the Web on November 24, 2015, with references 2−5 miscited throughout the paper. The corrected version was reposted on December 7, 2015.

DOI: 10.1021/acs.inorgchem.5b02105
Inorg. Chem. 2015, 54, 11457−11464